Supporting information

“Two in one”: an unprecedented mixed anions $Ba_2(C_3N_3O_3)(CNO)$ with the coexistence of isolated *sp* and sp^2 π-conjugated groups

Jian Tang,[a,c,#] Fei Liang,[b,d,#] Xianghe Meng,[b,d,#] Kaijin Kang,[a,c] Tixian Zeng,[c] Wenlong Yin*[a,e], Mingjun Xia,*[b,d] Zheshuai Lin[b] and Bin Kang[a]

[a]Institute of Chemical Materials, China Academy of Engineering Physics, Mianyang 621900, China. E-mail: E-mail: wlyin@caep.cn

[b]Beijing Center for Crystal Research and Development, Key Laboratory of Functional Crystals and Laser Technology, Technical Institute of Physics and Chemistry, Chinese Academy of Sciences, Beijing 100190, China. E-mail: xiamingjun@mail.ipc.ac.cn

[c]Physics and Space Science College, China West Normal University, Nanchong 637002, China

[d]Center of Materials Science and Optoelectronics Engineering, University of Chinese Academy of Sciences, Beijing 100049, China

[e]Key Laboratory of Science and Technology on High Energy Laser, China Academy of Engineering Physics, Mianyang 621900, China

1. Experimental methods

Solid state reaction

Mixture of KCNO and $BaCl_2$ with a molar ratio of 2 : 1 were thoroughly ground and placed in a fused-silica tube. The tube was flame-sealed under a high vacuum of 10^{-3} Pa and placed in a muffle furnace. Then furnace was heated to 873 K in 4 h and maintained for 72 h, and slowly cooled to room temperature at a rate of 3 K/h. Polycrystalline samples of **I** were obtained by washing the excess KCNO with dry ethanol.

Single crystal growth

The mixture of KCNO and $BaCl_2$ was placed in a fused-silica tube with a molar ratio of 2.5 :1 and the tube was flame-sealed under a high vacuum of 10^{-3} Pa, heated to 700 K in 6 h and held for 24 h at the temperature with several inter-grindings, then the pure phase powder of $Ba_3(C_3N_3O_3)_2$ was obtained. The pure phase powder of $Ba_3(C_3N_3O_3)_2$ was placed in a fused-silica tube and re-encapsulated under a high vacuum of 10^{-3} Pa. After that the ampoule was heated to 893 K within 5 h and held for 24 h and then slowly cooled to 423 K at a rate of 3 K/h. Finally, the ampoule was cooled to room temperature by switching off the furnace and small **I** crystals were obtained.

Structure determination

Single-crystal X-ray diffraction data for **I** were collected at room temperature on a Rigaku XtaLAB Synergy four-circle diffractometer equipped with a HyPix-6000HE area detector using Mo $K\alpha$ (PhotonJet-S Mo 50w Microfocus) radiation source. Data extraction and integration were carried out with use of the CrysAlisPro software. Structure solution and refinement were carried out with use of the SHELXTL (version 6.12) program package.[1] Initial atomic positions were located by direct methods and refinements proceeded in a straightforward fashion. All atomic sites were confirmed to be fully occupied and exhibited reasonable displacement parameters. No additional symmetry was revealed by the ADDSYM routine in the PLATON suite programs.[2]

Powder X-ray diffraction

Powder X-ray diffraction (PXRD) data were collected on a Bruker D8 Focus diffractometer equipped with Cu Kα radiation at room temperature in the 2θ range of 10 – 70°.

UV-vis-NIR diffuse reflectance spectrum

The spectrum of **I** was measured from 200 nm (6.2 eV) to 1800 nm (0.69 eV) on a Cary 7000 UV-vis-NIR spectrophotometer equipped with a diffuse reflectance accessory. A compacted pellet of $BaSO_4$ was used as a 100% reflectance standard. The absorption spectra were converted from reflectance spectra according to the Kubelka-Munk function: $\alpha/S = (1 - R)^2/2R$, where α, S and R are the absorption, scattering and reflectance coefficients, respectively.[3]

Infrared spectrum

Infrared (IR) spectroscopy was collected on a Varian Excalibur 3100 spectrometer in the 400 – 2400 cm^{-1} range. KBr and **I** samples with mass ratio about 100:1 were mixed thoroughly.

2. Computational method

The density functional theory calculations of **I** were performed in CASTEP package[4] by the plane-wave pseudo-potential methods. The total energy calculations including full structural optimizations were carried with the generalized gradient approximation with Perdew-Burke-Ernzerhof (PBE-sol) functional.[5] The optimized ultrasoft pseudopotentials[6] (Ba $4d^{10}6s^2$, C $2s^22p^2$, N $2s^22p^3$, O $2s^22p^4$) were used to simulate ion-electron interactions. A kinetic energy cutoff of 900 eV was chosen with Monkhorst-Pack *k*-point meshes (4×4×3) spanning less than 0.03/$Å^3$ in the first Brillouin zone.[7] The choice of these computational parameters is good enough to ensure the accuracy of the present purpose.[8, 9] Moreover, the linear response method was employed to obtain the phonon dispersion of crystal to evaluate its stability.[10] For phonon calculations, the ultrafine dispersion separation of 0.02/$Å^3$ and high cutoff energy of 1000 eV were adopted to make sure the good convergence. Finally, the elastic coefficients were also calculated and checked based on Born's stability criteria.[11]

Table S1. Crystal data and structure refinement for **I**.

Formula	$Ba_2(C_3N_3O_3)(CNO)$
Weight	442.7214
Temperature/K	293(2)
Crystal system	triclinic
Space group	$P\bar{1}$
a/Å	7.0743 (3)
b/Å	7.0882 (3)
c/Å	9.0679 (4)
α/°	82.146 (3)
β/°	75.303 (4)
γ/°	60.689 (4)
Volume/Å^3	383.47 (3)
Z	4
ρ_{calc}g/cm^3	3.835
μ/mm^{-1}	10.199
F(000)	392.0
Independent reflections	1565 [R_{int} = 0.0278]
Data/restraints/parameters	1565/0/128
Goodness-of-fit on F^2	1.076
Final R indexes [I>=2σ (I)]	R_1 = 0.0203, wR_2 = 0.0493
Final R indexes [all data]	R_1 = 0.0227, wR_2 = 0.0506

Table S2. Fractional atomic coordinates and isotropic or equivalent isotropic displacement parameters (Å) for **I**.

	x	y	z	Ueq
Ba1	1.37559(4)	0.81688 (4)	0.38351 (3)	0.01517(11)
Ba2	0.27272(4)	0.76676(4)	0.88043(3)	0.01540(11)
C1	0.9535(7)	0.3244(7)	0.7228(5)	0.0161(9)
C2	1.0985(7)	0.5604(7)	0.6553(5)	0.0122(8)
C3	0.7348(7)	0.6794(7)	0.6570(5)	0.0125(8)
C4	−0.2809(7)	0.7588(7)	1.0112(5)	0.0177(9)
N1	1.1327(6)	0.3588(6)	0.6984(5)	0.0172(8)
N2	0.9043(6)	0.7249(6)	0.6315(4)	0.0153(8)
N3	0.7493(6)	0.4847(6)	0.7049(5)	0.0164(8)
N4	−0.1626(6)	0.8417(6)	0.9755(5)	0.0181(8)
O1	0.5437(5)	0.8345(5)	0.6404(4)	0.0174 (7)
O2	1.2662(5)	0.5966(5)	0.6354(4)	0.0162(6)
O3	0.9692(6)	0.1396(6)	0.7666(5)	0.0306(9)
O4	−0.4016(6)	0.6829(7)	1.0474(5)	0.0381(10)

Table S3. Selected bond lengths (Å) and angles (degree) for **I**..

Ba1—O2	2.751(3)	Ba2—O4$^{\mathrm{viii}}$	2.882(4)
Ba1—O1$^{\mathrm{i}}$	2.766(3)	Ba2—N4$^{\mathrm{ix}}$	2.893(4)
Ba1—O2$^{\mathrm{ii}}$	2.772(3)	Ba2—N3	3.073(4)
Ba1—N2$^{\mathrm{i}}$	2.865(4)	C1—O3	1.275(6)
Ba1—O1$^{\mathrm{iii}}$	2.914(3)	C1—N1	1.364(5)
Ba1—N3$^{\mathrm{iv}}$	2.945(3)	C1—N3	1.366(6)
Ba1—O3$^{\mathrm{iv}}$	2.955(3)	C2—O2	1.297(5)
Ba1—N1$^{\mathrm{ii}}$	2.983(4)	C2—N2	1.344(6)
Ba1—O4$^{\mathrm{v}}$	3.092(4)	C2—N1	1.345(6)
Ba2—O1	2.672(3)	C3—O1	1.289(5)
Ba2—O2$^{\mathrm{vi}}$	2.689(3)	C3—N2	1.346(5)
Ba2—O3$^{\mathrm{vii}}$	2.735(3)	C3—N3	1.351(6)
Ba2—N4	2.772(3)	C4—O4	1.177(6)
Ba2—O4$^{\mathrm{iii}}$	2.852(4)	C4—N4	1.202(6)

O1—C3—N3	117.8(4)	N1—C1—N3	122.4(4)
O1—C3—N2	117.7(4)	N2—C2—N1	124.7(4)
O2—C2—N1	117.0(4)	N2—C3—N3	124.4(4)
O2—C2—N2	118.2(4)	C2—N1—C1	116.4(4)
O2—C2—N2	118.2(4)	C2—N2—C3	115.7(4)
O3—C1—N1	120.9(4)	C3—N3—C1	116.3(4)
O3—C1—N3	116.8(4)	O4—C4—N4	178.2(5)

Symmetry codes: (i) −*x*+2, −*y*+2, −z+1; (ii) −*x*+3, −*y*+1, −z+1; (iii) *x*+1, *y*, *z*; (iv) −*x*+2, −*y*+1, −z+1; (v) *x*+2, *y*, *z*−1; (vi) *x*−1, *y*, *z*; (vii) *x*−1, *y*+1, *z*; (viii) −*x*, −*y*+1, −*z*+2; (ix) −*x*, −*y*+2, −z+2.

Table S4. The calculated elastic constants C_{ij} (GPa) of **I**..

i \ **j**	1	2	3	4	5	6
1	63.8924	39.96615	4.2308	-2.10393	17.50037	-0.36633
2	39.96615	93.61405	23.81915	-11.594	0.13227	1.842
3	4.2308	23.81915	22.5861	8.33638	7.7036	-1.72237
4	-2.10393	-11.594	8.33638	11.197	0.39155	6.09252
5	17.50037	0.13227	7.7036	0.39155	5.53185	-2.90418
6	-0.36633	1.842	-1.72237	6.09252	-2.90418	31.35245

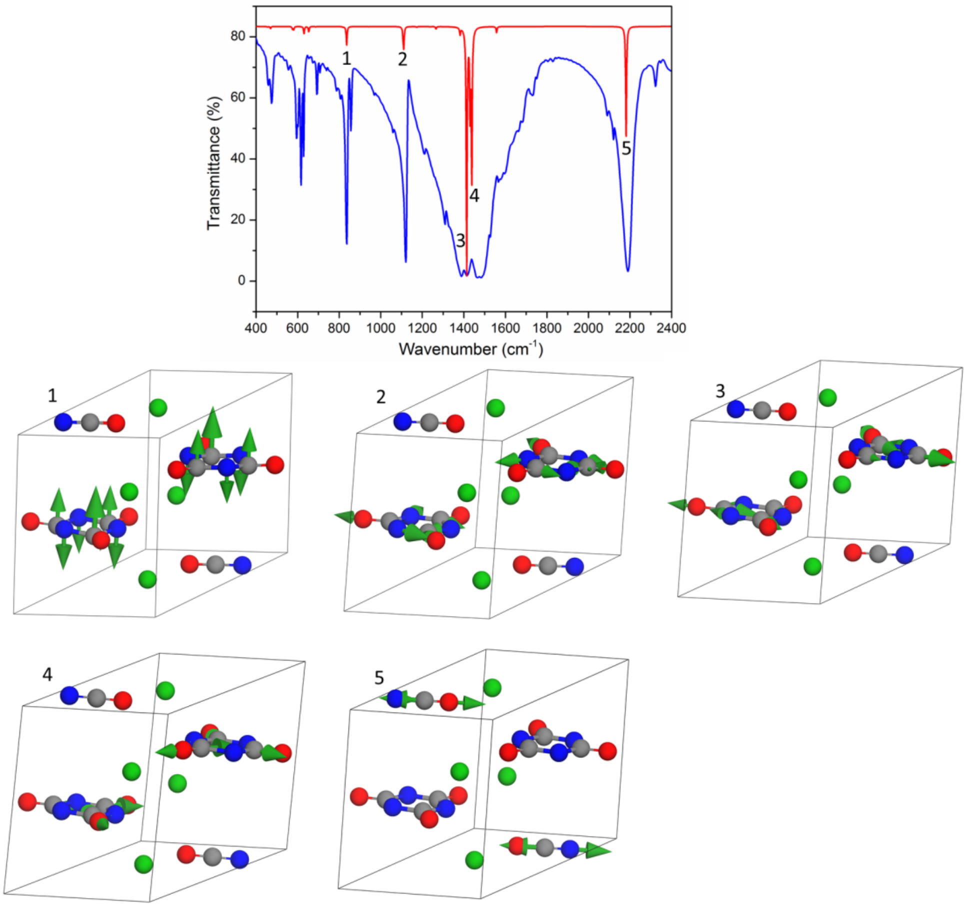

Figure S1. The infrared spectrum of **I** and corresponding vibrational modes simulated by phonon calculations. Figures 1 - 4 show that the peaks at 846, 1120, 1423 and 1448 cm^{-1} can be assigned to intrinsic modes of planar $(C_3N_3O_3)^{3-}$ 6-MR. Figure 5 represents the peak at 2191 cm^{-1} is related to stretching mode of $(CNO)^{-}$ chain.

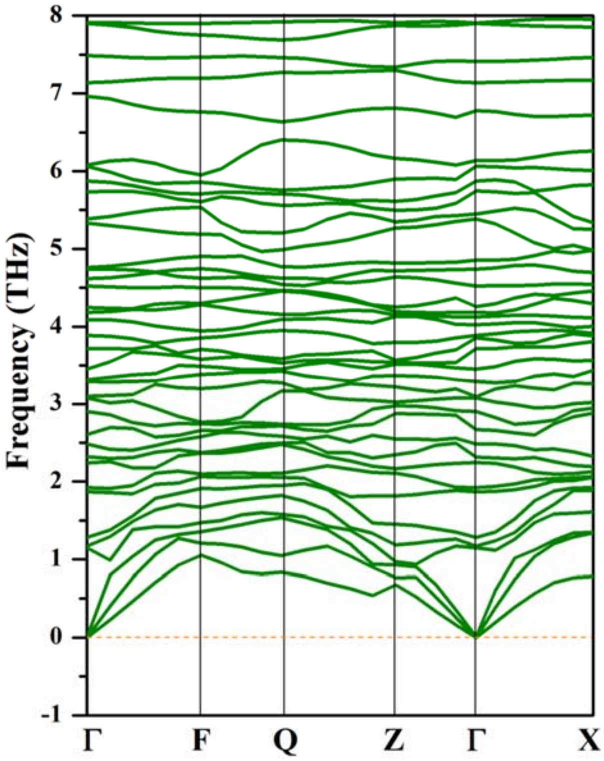

Figure S2. The phonon spectrum of **I**.

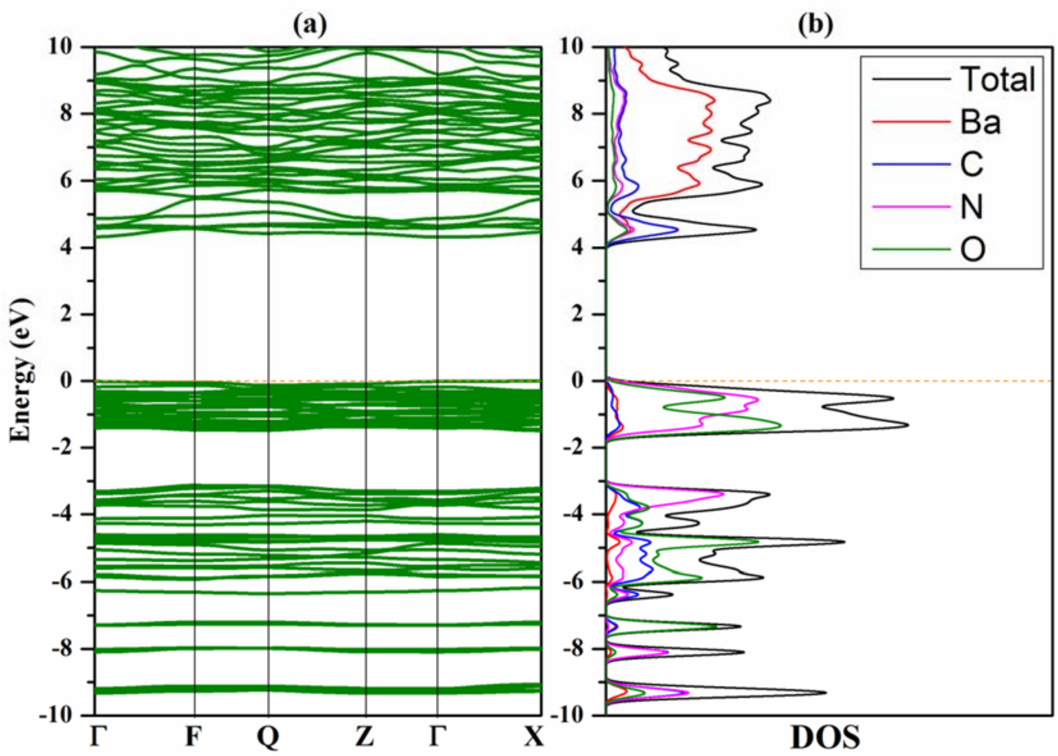

Figure S3. (a) Electronic band structure and (b) density of states of **I** calculated by the PBE functional.

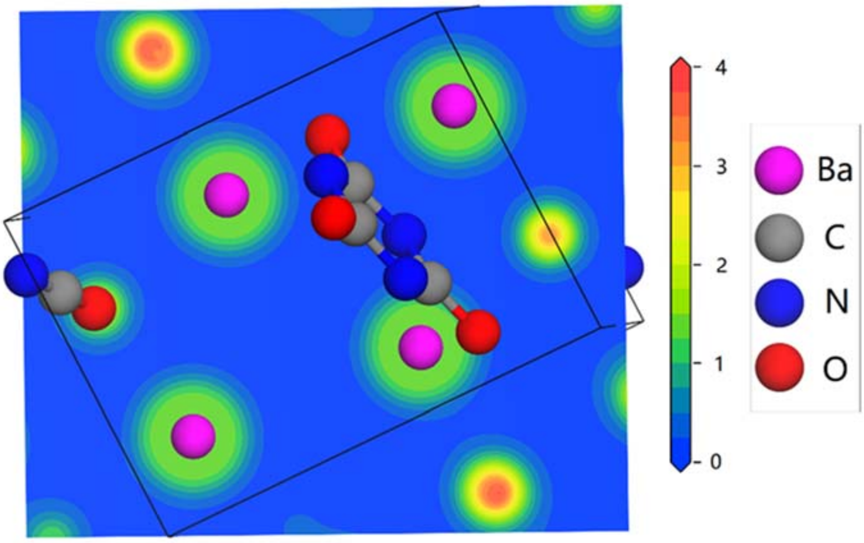

Figure S4. The electron distribution map of **I**.

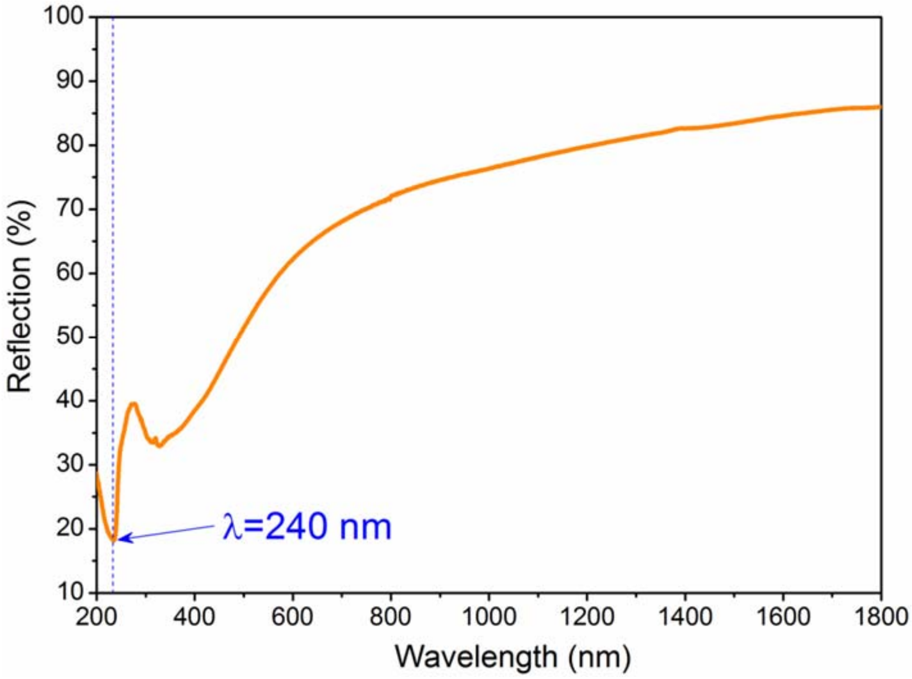

Figure S5. The reflectance spectrum of **I** in the range of 200 - 1800 nm.

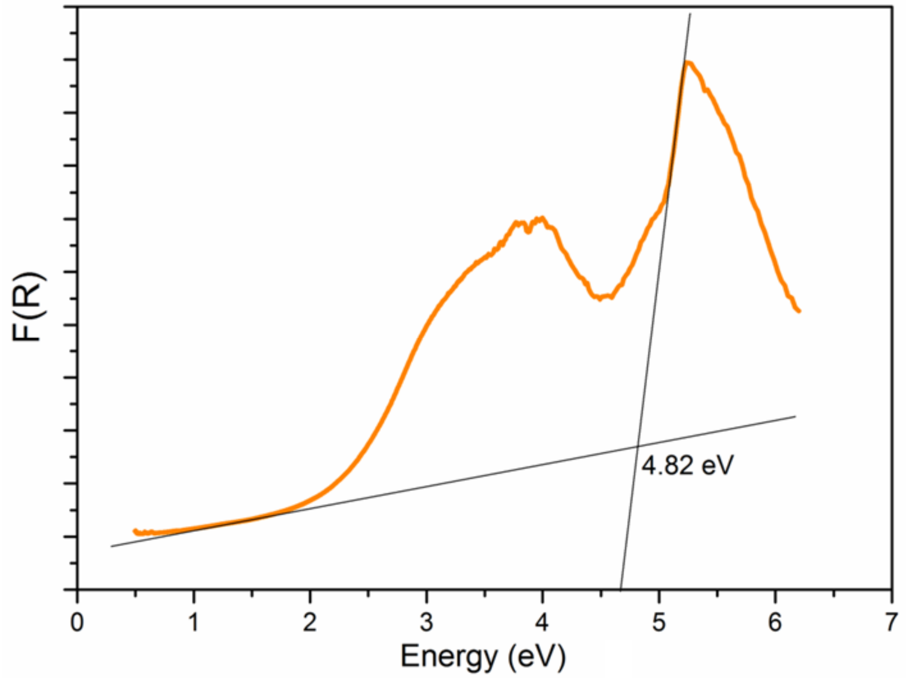

Figure S6. The band gap of **I**.

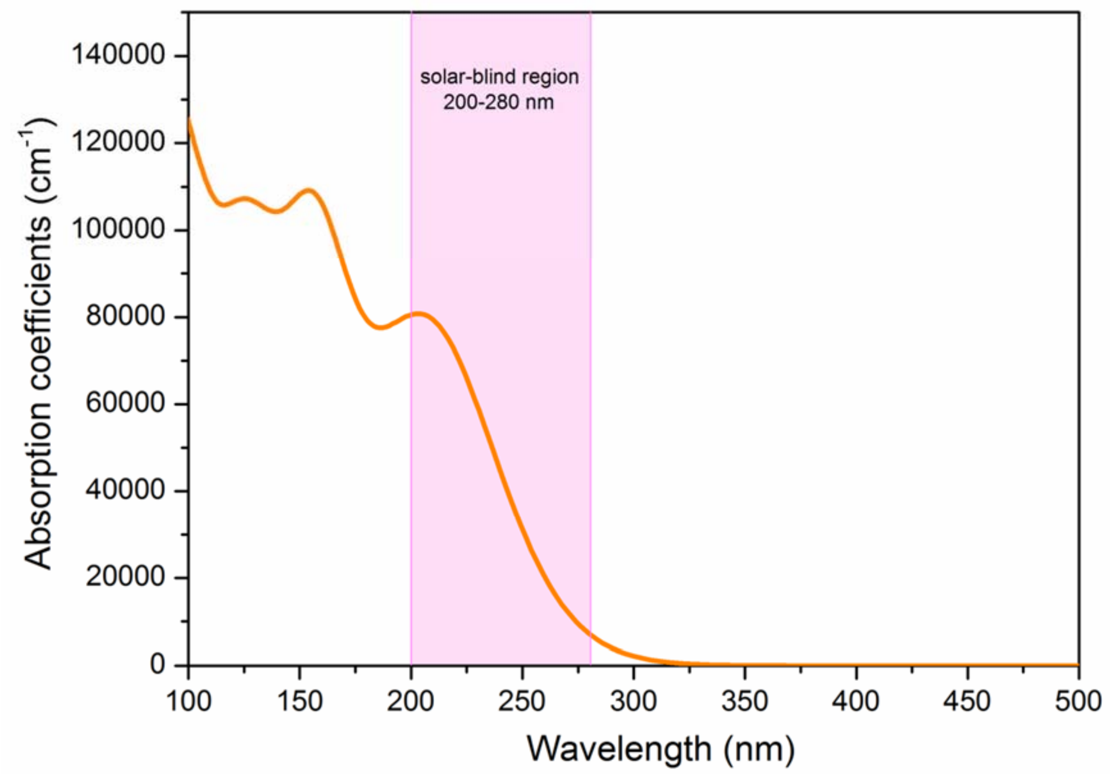

Figure S7. The simulated absorption coefficients of polycrystalline **I**. The band gap has been corrected by scissor operator of 0.5 eV.

References

1. Sheldrick, G. M., Crystal structure refinement with SHELXL. *Acta Crystallogr., Sect. C: Struct. Chem.* **2015,** *71*, 3-8.

2. Spek, A. L., Single-crystal structure validation with the program PLATON. *J. Appl. Crystallogr.* **2003,** *36*, 7-13.

3. Loyalka, S. K.; Riggs, C. A., Inverse Problem in Diffuse-Reflectance Spectroscopy: Accuracy of the Kubelka-Munk Equations. *Appl. Spectrosc.* **1995,** *49*, 1107-1110.

4. Clark, S. J.; Segall, M. D.; Pickard, C. J.; Hasnip, P. J.; Probert, M. J.; Refson, K.; Payne, M. C., First Principles Methods Using CASTEP. *Z. Kristallogr.* **2005,** *220*, 567-570.

5. Perdew, J. P.; Burke, K.; Ernzerhof, M., Generalized Gradient Approximation Made Simple. *Phys. Rev. Lett.* **1996,** *77*, 3865-3868.

6. Rappe, A. M.; Rabe, K. M.; Kaxiras, E.; Joannopoulos, J. D., Optimized Pseudopotentials. *Phys. Rev. B* **1990,** *41*, 1227-1230.

7. Monkhorst, H. J.; Pack, J. D., Special Points For Brillouin-Zone Integrations. *Phys. Rev. B* **1976,** *13*, 5188-5192.

8. Liang, F.; Kang, L.; Zhang, X.; Lee, M.; Lin, Z.; Wu, Y., Molecular Construction Using $(C_3N_3O_3)^{3-}$ Anions: Analysis and Prospect for Inorganic Metal Cyanurates Nonlinear Optical Materials. *Cryst. Growth & Des.* **2017,** *17*, 4015-4020.

9. Xia, M.; Zhou, M.; Liang, F.; Meng, X.; Yao, J.; Lin, Z.; Li, R., Noncentrosymmetric Cubic Cyanurate $K_6Cd_3(C_3N_3O_3)_4$ Containing Isolated Planar π-Conjugated $(C_3N_3O_3)^{3-}$ Groups. *Inorg. Chem.* **2018,** *57*, 32-36.

10. Baroni, S.; de Gironcoli, S.; Dal Corso, A.; Giannozzi, P., Phonons and Related Crystal Properties from Density-functional Perturbation Theory. *Rev. Mod. Phys.* **2001,** *73*, 515-562.

11. Liu, Q.; Ran, Z.; Liu, F.; Liu, Z., Phase Transitions and Mechanical Stability of TiO_2 Polymorphs under High Pressure. *J. Alloys Compd.* **2015,** *631*, 192-201.